

## An Overview of the China Meteorological Administration Tropical Cyclone Database

MING YING, WEI ZHANG, HUI YU, XIAOQIN LU, AND JINGXIAN FENG

*Shanghai Typhoon Institute, China Meteorological Administration, Shanghai, China*

YONGXIANG FAN

*National Meteorological Center, China Meteorological Administration, Beijing, China*

YONGTI ZHU AND DEQUAN CHEN

*Shanghai Typhoon Institute, China Meteorological Administration, Shanghai, China*

(Manuscript received 18 May 2012, in final form 4 July 2013)

### ABSTRACT

The China Meteorological Administration (CMA)'s tropical cyclone (TC) database includes not only the best-track dataset but also TC-induced wind and precipitation data. This article summarizes the characteristics and key technical details of the CMA TC database. In addition to the best-track data, other phenomena that occurred with the TCs are also recorded in the dataset, such as the subcenters, extratropical transitions, outer-range severe winds associated with TCs over the South China Sea, and coastal severe winds associated with TCs landfalling in China. These data provide additional information for researchers. The TC-induced wind and precipitation data, which map the distribution of severe wind and rainfall, are also helpful for investigating the impacts of TCs. The study also considers the changing reliability of the various data sources used since the database was created and the potential causes of temporal and spatial inhomogeneities within the datasets. Because of the greater number of observations available for analysis, the CMA TC database is likely to be more accurate and complete over the offshore and land areas of China than over the open ocean. Temporal inhomogeneities were induced primarily by changes to the nature and quality of the input data, such as the development of a weather observation network in China and the use of satellite image analysis to replace the original aircraft reconnaissance data. Furthermore, technical and factitious changes, such as to the wind–pressure relationship and the satellite-derived current intensity (CI) number–intensity conversion, also led to inhomogeneities within the datasets.

### 1. Introduction

Four agencies issue tropical cyclone (TC) best-track datasets for the western North Pacific (WNP) basin. In addition to the World Meteorological Organization (WMO) Regional Specialized Meteorological Center (RSMC) in Tokyo, Japan, best-track datasets are issued by the Joint Typhoon Warning Center (JTWC) of the U.S. Navy, the China Meteorological Administration (CMA), and the Hong Kong Observatory (HKO). All four

best-track datasets are included in the International Best Track Archive for Climate Stewardship (IBTrACS) project (Knapp et al. 2010), which is an official WMO global archiving and distribution resource for TC best-track data. An increasing number of researchers are using IBTrACS as the basic data source for their studies (e.g., Dare and McBride 2011; Diamond et al. 2013; Ying et al. 2012). However, many authors have suggested that the global best-track data may be inhomogeneous in both time and space (Emanuel 2005; Landsea et al. 2006; Levinson et al. 2010), and this is primarily caused by nonclimatic changes (see Peterson et al. 1998) as well as the differences in such changes from basin to basin. Even within the same basin, differences among the various agencies are remarkable. Taking the WNP basin as an example, the four best-track datasets are inconsistent in various aspects, including wind averaging times (Holland

---

 Denotes Open Access content.

---

*Corresponding author address:* Dr. Ming Ying, Shanghai Typhoon Institute, China Meteorological Administration, 166 Puxi Road, Xuhui District, Shanghai 200030, China.  
E-mail: yingm@mail.typhoon.gov.cn

DOI: 10.1175/JTECH-D-12-00119.1

1993), Dvorak parameters (Nakazawa and Hoshino 2009), storm position and intensity (Hoarau et al. 2006; Lander and Guard 2006; Lei 2001; Yu et al. 2007, 2012), and climatology and variabilities (Kwon et al. 2006; Lander 2008; Lee et al. 2012; Wang et al. 2008; Wu et al. 2006; Ying et al. 2011a).

Although TC best-track data issues have been discussed frequently, there remains a lack of knowledge regarding the processes used to generate these datasets, and this may be an obstacle to the use of these data. With the support of the United Nations Economic and Social Commission for Asia and the Pacific (ESCAP) and the WMO Typhoon Committee, the Tropical Cyclone Best Track Consolidation Meeting was held in Hong Kong, China, on 13–14 December 2010. Experts from the RSMC Tokyo, JTWC, the Shanghai Typhoon Institute (STI) of the CMA, and HKO exchanged detailed information on best-track analysis and reached agreement regarding ongoing efforts to reduce the discrepancies among the agencies. We believe that an overview of the best-track dataset at this point will provide a necessary and helpful first step; consequently, this paper summarizes the history and technical development of the CMA TC database.

In response to a request for increased forecasting and research activity in China, a TC reanalysis project was sponsored between 1969 and 1972. Meteorologists and experts from within and outside the CMA were brought together by this project, and focused on the construction of the official CMA TC database, which included the best-track data and TC-induced wind and precipitation observations for TC seasons 1949–71. Following the completion of this project, annual postseason analysis, rather than real-time analysis, was used to construct the CMA TC database for five reasons. First, the real-time analysis only covered the western section of the WNP basin (105°–150°E) prior to 1986. Second, the quality control of the data used in real-time analysis is not as rigorous as that for the archived data, which are the data used for the postseason analysis. Third, the postseason analysis handles a TC event as a whole process and verifies each TC data record with several adjacent records, thereby reducing uncertainties and errors. Fourth, the tropical depression (TD) cases were outside the scope of real-time analysis over the past several decades. Fifth, the procedure for constructing the TC-induced wind and precipitation data is too complex for real-time operation. Moreover, the real-time and postseason analyses at the CMA are the independent responsibilities of different institutions, an arrangement that differs from that at other agencies. The former is one of the responsibilities

of the National Meteorological Center (NMC)<sup>1</sup> of the CMA, while the latter, in contrast, was initially (since 1972) part of the routine work of the Shanghai Meteorological Service/CMA (with the endorsement of the CMA), but in 1981 became one of the responsibilities of the STI/CMA. Fortunately, several of the expert team members from the reanalysis project continued to work on the database during the post-season analysis era. Now, the STI/CMA has archived more than 60 years of TC activity data, including not only the best-track data covering the WNP and South China Sea (SCS) region (0°–55°N, 105°E–180°) but also the TC-induced wind and precipitation data covering the land area of China.

The basic contents of the CMA TC database, as well as the main procedures and analysis rules, have changed little since they were designed and fixed during the reanalysis project. However, the input data used in analysis, and the technical details of the analytical procedures, have changed several times, especially since the start of the postseason analysis era. An overview of these related issues may be useful to those using the database. In this paper, we summarize the basic features of, and changes to, the CMA TC database since its creation. The contents of both datasets, which hold the best-track data and TC-induced wind and precipitation data, are summarized in section 2. An overview of the input data and technical details is provided in section 3. Finally, concluding remarks are presented in section 4.

## 2. Contents of the CMA TC database

As mentioned above, the CMA TC database includes two parts: the best-track dataset and its supplementary data, and the TC-induced wind and precipitation observation dataset for the land area of China. Both datasets cover seasons from 1949 to the present, and are updated annually.

### a. CMA best-track dataset

The CMA TC best-track dataset (Table 1) contains the basic-track information for all identified TCs,

---

<sup>1</sup>The NMC/CMA began its real-time TC track analysis in 1959. Its area of responsibility covered the western area of the WNP (105°–150°E) during the period 1959–85, and was enlarged to the whole WNP basin in 1986. The NMC designates the CMA identification number (ID) for each TC that forms in, or enters, its area of responsibility when the TC either reaches maximum sustained wind (MSW)  $\geq 17.2 \text{ m s}^{-1}$  over the open ocean or  $\text{MSW} \geq 13.9 \text{ m s}^{-1}$  over the area offshore of China. For these TCs, the NMC also issues the real-time track analysis (including location and intensity) until they decay or move out of the area of responsibility.

TABLE 1. Summaries of the four available TC best-track datasets for the western North Pacific basin.

Agency	Data period	Contents	Wind averaging period (min)	Website
CMA	1949–current	1) Longitude, latitude, MSW, and MSLP back to 1949 2) Extratropical stage back to 1949 3) Subcenters, outer-range cases over the SCS, and coastal severe winds of landfalling TCs	2	<a href="http://tcdata.typhoon.gov.cn/en/index.html">http://tcdata.typhoon.gov.cn/en/index.html</a>
HKO	1961–current	Longitude, latitude, MSW, and MSLP back to 1961	10	<a href="http://www.hko.gov.hk/publica/pubtc.htm">http://www.hko.gov.hk/publica/pubtc.htm</a>
JTWC	1945–current	1) Longitude, latitude, and MSW back to 1945 2) Extratropical cyclone stage back to 2004, and MSLP and TC size parameters back to 2001	1	<a href="http://www.usno.navy.mil/NOOC/nmfc-ph/RSS/jtwc/best_tracks/">http://www.usno.navy.mil/NOOC/nmfc-ph/RSS/jtwc/best_tracks/</a>
RSMC Tokyo	1951–current	1) Longitude, latitude, MSLP, and markers for both the TS stage and landfall time back to 1951 2) Extratropical cyclone stage, MSW, and typical severe wind radii back to 1977	10	<a href="http://www.jma.go.jp/jma/jma-eng/jma-center/rsmc-hp-pub-eg/trackarchives.html">http://www.jma.go.jp/jma/jma-eng/jma-center/rsmc-hp-pub-eg/trackarchives.html</a>

including TD cases, which typically generate heavy rainfall over southern China.

The basic-track information is similar to that in the datasets of the other agencies, and includes location, MSW, and minimum sea level pressure (MSLP). However, the CMA is unique in using MSW obtained from a 2-min mean. The technical aspects regarding the 2-min mean MSW will be discussed in section 3b. The CMA best-track dataset also focuses on specific phenomena, such as extratropical cyclone stages, subcenters, the outer-range severe winds of TCs over the SCS, and coastal severe winds associated with TCs landfalling in China. In addition, specialized landfalling TC data and satellite imagery analysis data are included as supplements to the best-track data. In the following sections, we introduce this special content of the CMA best-track dataset.

### 1) EXTRATROPICAL TRANSITION

The extratropical cyclone stage indicates the end of the extratropical transition (ET) process when the midlatitude front system has merged into the inner core of TC circulation. The record for the extratropical cyclone stage includes the storm's central location, MSW, and MSLP every 6 h, which are the same as for the standard TC track record.

### 2) THE SUBCENTER

The subcenter is a special phenomenon only recorded in the CMA best-track dataset; it is a circulation center accompanied by a warm core, which is defined using the

same synoptic charts and data as for the best-track analysis (see section 3b). The subcenters usually split from, or are induced by, the parent TC circulation (Shanghai Typhoon Institute 1990), and generally result from a TC interacting with either the topography or other synoptic systems, or from the reintensification of a decayed TC vortex under favorable conditions. In some cases, a subcenter can move a considerable distance from the parent TC and subsequently develop into a storm with  $MSW \geq 17.2 \text{ m s}^{-1}$ . Approximately 40 TCs generating 1–3 subcenters have been recorded in the dataset. The 40 cases can be classified into three groups. First, a subcenter that is reintensified from a decayed TC vortex can be considered as a special stage of its parent TC. Similarly, a subcenter that is induced by its parent TC and that develops or is maintained for a period as the parent quickly decays can also be considered an extension of the parent TC. Such cases include Nora (1959), Wendy (1963), Andy (1982), Alex (1984), Polly (1992), and Winnie (1997). Second, some subcenters split from, or are induced by, the parent TC and develop into or maintain an intensity of TS category; meanwhile, the parent TC persists for a significant period. Such subcenters can be considered to be newly generated storms and examples include Trix (1960) and Faye/Gloria (1971). Third, some subcenters are weak and decay quickly and can be excluded from the climate statistics.

For example, Fig. 1 shows Typhoon Dot (1990) and its two subcenters. At 1200 UTC 7 September 1990, the first subcenter was generated on the western side of the Central Mountain Range of Taiwan as Dot was

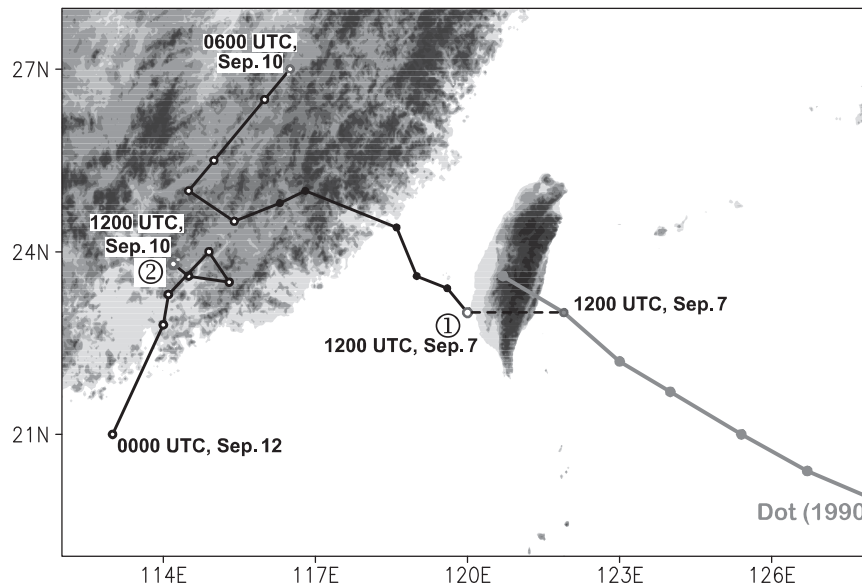


FIG. 1. Tracks of Typhoon Dot (1990) (gray solid line) and its two subcenters (black solid lines) marked ① and ②, respectively. Solid dots indicate  $MSW \geq 17.2 \text{ m s}^{-1}$ , and open dots indicate  $MSW < 17.2 \text{ m s}^{-1}$ . Dashed lines indicate the coexistence of double centers. Shading of land areas is proportional to the elevation (e.g., higher elevations are darker).

approaching the island (as indicated by the black solid line in Fig. 1). During the next 6 h, the MSW of the parent circulation decreased from  $40$  to  $35 \text{ m s}^{-1}$ , and it later dissipated. Meanwhile, the first subcenter moved westward and its MSW increased from  $15$  to  $35 \text{ m s}^{-1}$ . As suggested by Meng et al. (1996), the influence of topography on Dot might have been an important control on the location and intensity of the subcenter. After the first subcenter made landfall on mainland China, it moved inland and was affected by the Nanling Mountains of southern China. The second subcenter was generated at  $23.8^\circ\text{N}$ ,  $114.2^\circ\text{E}$  about 6 h after the first subcenter dissipated at  $27.0^\circ\text{N}$ ,  $116.5^\circ\text{E}$ . The circulation and upper-level warm core associated with the subcenters of Dot (1990), based on the Japanese 25-year Reanalysis Project (JRA-25) data (Onogi et al. 2007), are shown in Fig. 2. Although the JRA-25 dataset was not used to define the subcenter, its resolution is relatively coarse ( $1.25^\circ \times 1.25^\circ$ ), and the dataset is based on the RSMC Tokyo best-track dataset, the typical structure of the subcenter, such as the low-level circulation and warm core, is well represented. The left and right panels of Fig. 2 are for 0600 and 1800 UTC 10 September 1990, respectively; that is, the panels show the 6-h pregenesis and postgenesis of the second subcenter, respectively. Figures 2a–c indicate the structure of the first subcenter, which is consistent with the measured MSW of  $10 \text{ m s}^{-1}$ . In particular, the outflow and warm core are clear at 300 hPa, and the cyclonic circulation is clear at

500 and 925 hPa. However, the cyclonic circulation is elongated on its north and south sides, which may be favorable for the genesis of the second subcenter. Later, 6 h after the generation of the second subcenter, the outflow and warm core are still obvious at 300 hPa, but the cyclonic circulation at 500 hPa is less distinct than that observed 12 h before, while the near-surface cyclonic circulation remains clear (Figs. 2d–f). Note that it appears that the near-surface circulation center is some distance from the surface center (Fig. 2f). This may be due to the discrepancies between station observations and the model-produced reanalysis data.

### 3) OUTER-RANGE AND COASTAL SEVERE WINDS

In addition to the ordinary MSW data used as a parameter of TC intensity, there is a special wind speed parameter  $m$  in the CMA best-track data. This parameter ( $m$ ) is related to two forms of special phenomena: outer-range severe winds associated with some TCs over the SCS and the coastal severe winds associated with some landfalling TCs. Both phenomena have been associated with TCs and related disasters (e.g., casualties and damage to fishing boats), especially during the early years.

The outer-range severe wind is a special phenomenon associated with some TCs located over the SCS (Chen and Ding 1979). For those cases with outer-range severe winds, the additional parameter  $m$  denotes the maximum outer-range severe wind speed within a radius of

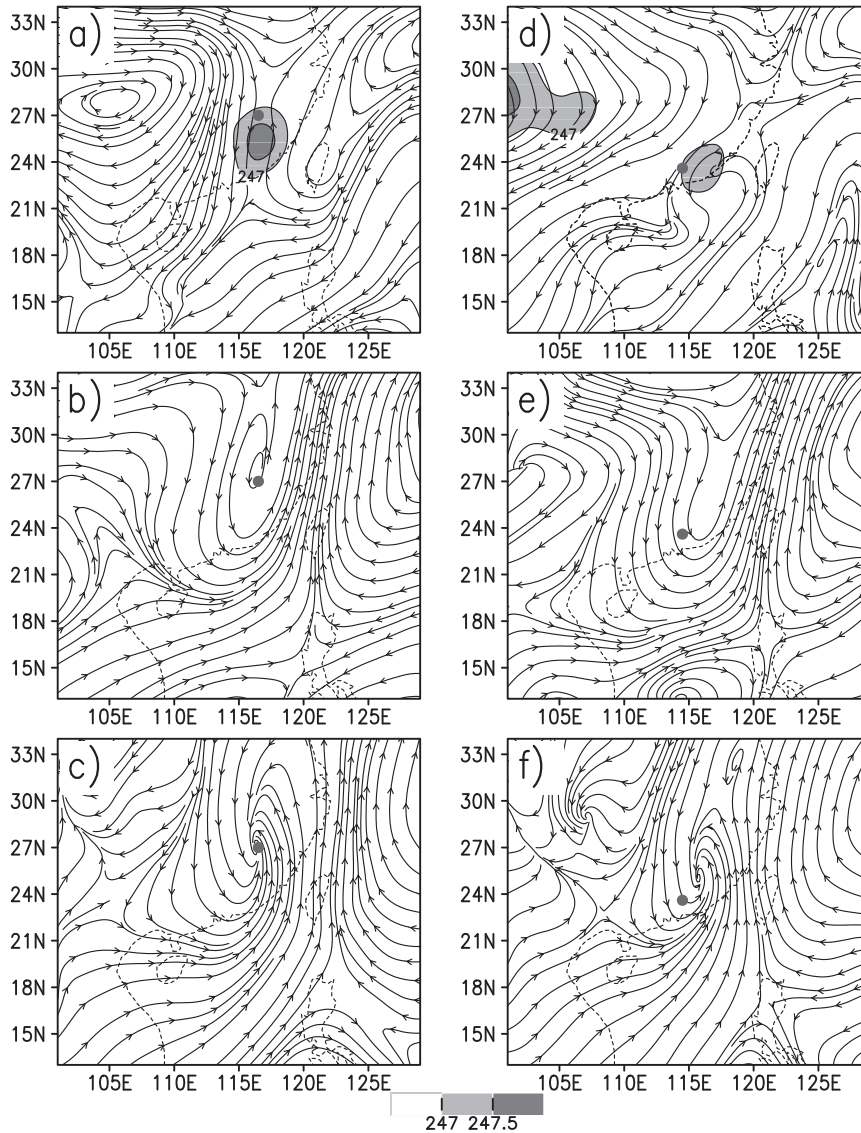


FIG. 2. Temperature (K, shaded) and wind stream at (left) 0600 and (right) 1800 UTC 10 Sep 1990: (a),(d) 300, (b),(e) 500, and (c),(f) 925 hPa. Solid dots indicate the corresponding best-track locations of the subcenters.

approximately 300–500 km from the TC center, which is outside the MSW. Although the CMA TC database only includes a small number of such cases, these cases provide observational evidence for the special evolution of SCS TCs. For example, Fig. 3a shows the intensity evolution of Tropical Storm (TS) 7823, and its associated outer-range severe wind develops between 1800 UTC 31 October and 1800 UTC 1 November. Following this stage, the storm intensified.

Some TCs that make landfall in China may generate a severe wind zone along the coastline, with winds even stronger than their MSWs (Chen and Ding 1979). Such phenomena usually occur when a TC interacts with

a warm depression over the landmass. In these cases, the additional parameter  $m$  denotes the maximum coastal severe wind, which is farther away from the TC center than the MSW. Figure 3b shows the intensity evolution of a typical landfalling case with a coastal severe wind: Typhoon Gilda (1952). Unlike the evolution of outer-range severe winds, the MSW and coastal severe wind weakened step by step as Gilda (1952) moved inland, and hence farther from the coastline. This is a typical feature of landfalling TCs accompanied by a severe coastal wind.

As these two forms of severe wind phenomena are represented in the same format in the dataset, a convenient method of distinguishing between them is to check

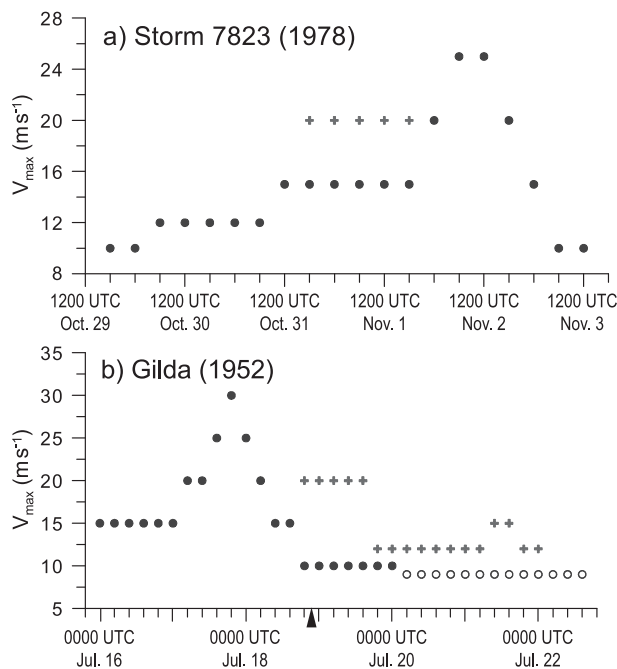


FIG. 3. Intensity evolution for (a) TS 7823 and (b) TY Gilda (1952). In (a), the solid dots denote MSW, while the “+” symbol denotes the outer-range wind speed at a radius of 300–500 km from the TC center. In (b), the solid dots denote the MSW, while the “+” symbol denotes coastal severe wind, and open dots denote  $MSW < 10 \text{ m s}^{-1}$ . The triangle in (b) indicates the time of Gilda’s landfall in China.

the location of the TC; that is, outer-range severe winds are restricted to TCs over the SCS, while coastal severe winds only occur when the TC moves over the land area of China.

#### 4) LANDFALLING TC DATA

As a supplement to the best-track dataset, the CMA TC database also includes specialized data for TCs that made landfall in China from the 1949 season to the present. A sample of the landfalling TC data is shown in Table 2. The data include the TC ID, landfall event, location, date and time, and TC intensity at the time of

landfall in China. The TC ID is the same as that in the best-track dataset. The landfall times indicate how many times a TC made landfall in China, including on the Zhoushan Archipelago (in the East China Sea), the large islands of Hainan (in the SCS), and Taiwan. For instance, the severe TS Otto (1998), marked with CMA ID 9802, made landfall in China twice: first in Taiwan and then in Fujian Province (Table 2). Landfall intensity is determined using three measures: the Beaufort scale (BS) for wind strength, MSW, and MSLP. It should be noted that both the BS and MSLP data are available back to the 1949 season, and the MSW data are available back to the 1973 season.

#### 5) SATELLITE IMAGE ANALYSIS

A further addition to the CMA best-track dataset is the archive of real-time (i.e., not the “best analysis”) satellite image analysis data, covering the TC seasons from 1985 to 2004. These supplementary data include date and time, location, location-fix error, intensity, diameter of dense cloud cover, intensity change during the past 24 h, time interval for the translation estimation, and translation speed and direction. The intensity includes the current intensity (CI) number (Dvorak 1975) and MSW.

#### 6) ADDITIONAL FEATURES

As well as the additional data mentioned above, some of the general content of the CMA best-track dataset also makes it distinct from other similar datasets (Table 1). For instance, the MSW in the RSMC Tokyo data is undefined for seasons 1951–76, while the life stages of storms in the TS category or higher are recorded. The MSLP in the JTWC data is undefined for TC seasons from 1945 to 1999. TD cases and extratropical cyclone stages (see sections 2a and 3b) are not recorded in the RSMC Tokyo and HKO data, respectively. However, the CMA dataset does not contain some content that is included in the other datasets, such as the TC size

TABLE 2. Landfalling TC data for the 1998 season. Serial number (SN) and CMA ID (CN) for a particular case. The date and time are local time (Beijing time, “mm” denotes two-digit month, “dd” two-digit day, “hh” two-digit hour, and “nn” two-digit minute), which leads Greenwich standard time by 8 h.

SN	ID CN	Landfall events		Location of landfall (County, Province)	Date and time (mmddhhnn)	Intensity at landfall		
		Total	No.			BS	$\text{m s}^{-1}$	hPa
1	9801	1	1	Tainan, Taiwan	07100100	8	18	998
3	9802	2	1	Xin’gang, Taiwan	08041200	11	30	980
3	9802	2	2	Fuqing, Fujian	08050200	8	18	998
4	9803	1	1	Yangjiang, Guangdong	08110730	10	25	990
5	—	1	1	Xuwen–Haikang, Guangdong	08221900	7	14	1002
8	—	1	1	Wenchang, Hainan	09131500	7	15	1000
10	9806	1	1	Putuo, Zhejiang	09192230	10	25	985

parameter in both the RSMC Tokyo and JTWC datasets, and an indicator for the time of TCs landfalling on Japan in the RSMC Tokyo dataset.

### *b. CMA TC-induced wind and precipitation dataset*

The TC-induced wind and precipitation data are also important components of the CMA TC database. The dataset includes the statistics for TC-induced wind and precipitation observations, TC IDs, the date and duration of the TC's influence on China, and the total number of stations affected by TCs.

For each station, the TC-induced wind data contain the date and duration of wind speeds observed to be greater than or equal to BS 8 and both the extreme sustained wind and extreme gust with associated directions. For the wind duration, a day is defined as 0000–2359 UTC, and the extreme wind is recorded in 1 of the 16 standard directions. The TC-induced precipitation data contain daily precipitation, maximum 1-h precipitation, and the associated date and time. For the duration and daily amount of precipitation, a day is defined as 0000–2359 UTC for the 1949–84 seasons, but from 1200 to 1159 UTC for the TC seasons from 1985 to the present.

## **3. Analysis of the CMA TC data**

As mentioned in section 1, the CMA TC data can be divided into two stages: the first is the reanalysis stage for the seasons from 1949 to 1971 and the second is the annual postseason analysis stage for TC seasons from 1972 to the present. The first difference between the best-track and real-time analysis is that the coverage area of the real-time analysis was limited to the western area of the WNP basin before 1986, while the best-track data covers the whole basin back to the 1949 season. The second difference is that the TD cases are usually beyond the scope of real-time analysis but are included in the best-track data. The raw data inputs and procedures for the CMA TC “best” data are as follows.

### *a. Raw data inputs*

As shown in Fig. 4, the data used for the 1949–71 seasons, which are the products of the CMA reanalysis project (1969–72), included historical atlases of TC tracks (e.g., Gao and Zeng 1957; and those mentioned in Wang 1997), station observations and ship weather reports, automated surface observations, synoptic charts, radiosonde data, aircraft reconnaissance, and real-time TC warning advice from various agencies. Note that imagery from both satellite and coastal radar were not used during this era. In contrast, the data used during TC seasons since 1972, which are products of the annual routine postseason analysis, include not only the

observations used in the reanalysis era but also satellite and coastal radar observations. It is worth mentioning that the MSLP and MSW estimates from the aircraft reconnaissance data were used without any further quality control.

Figure 4 indicates that fewer changes were made to the input data used in the reanalysis era (1949–71) than during the annual postseason analysis era (1972–present). However, inhomogeneities may also be attributed to changes in the input data as the observation network was developed. In particular, over the land area of China, the number of stations increased dramatically during the 1950s, especially during the early 1950s (e.g., Ying and Wan 2011). A noticeable change also occurred in 2007, when the number of stations increased from around 1600 to more than 2100 (Fig. 5). Moreover, the radar network, which is especially useful for TCs over the offshore area of China, has also developed steadily during the postseason analysis era, from the C-band (at wavelengths around 5 cm) radar network in the 1970s to the S-band (at wavelengths around 10 cm) radar in the 1980s. The Doppler radar network has developed since the 1990s. Now, the Doppler radar network ([http://www.weather.com.cn/static/en\\_product.php?class=JC\\_RADAR\\_CHN\\_JB](http://www.weather.com.cn/static/en_product.php?class=JC_RADAR_CHN_JB)) covers all of the land area affected by TCs (Xu 2006) and the offshore area of China. It seems reasonable to assume that these changes had some effect on the inhomogeneities within the data, especially the best-track data, landfalling TC data, and TC-induced wind and precipitation data.

Over the open ocean, aircraft reconnaissance missions covered the TC data period from 1949 to 15 August 1987 (Reade 2011). However, few reconnaissance data were collected for analyzing the best track in the early 1950s. Following the end of aircraft reconnaissance in 1987, a growing collection of satellite data, with an increasing resolution and expanding number of missions, has been used instead (Fig. 4). These changes may influence the best-track data over the open ocean, especially the extreme intensity values, due to the limitation of statistical satellite image analysis techniques (Dvorak 1975; Group of Satellite Imagery Analysis 1980a,b). Figure 6 shows the annual occurrence frequency of MSW values for TCs in the CMA best-track dataset. For TCs over the open ocean (Fig. 6a), the occurrence frequency of MSWs above  $60 \text{ m s}^{-1}$  is dramatically lower during the period 1988–2010 when compared with 1965–87. Similarly, for TCs close to land (including islands) (Fig. 6b), the occurrence frequency of MSWs greater than  $60 \text{ m s}^{-1}$  also decreases, but the change is not as significant as that over the open ocean. This may result from both the errors in reconnaissance wind estimates in the 1950s and the replacement of aircraft reconnaissance data by satellite

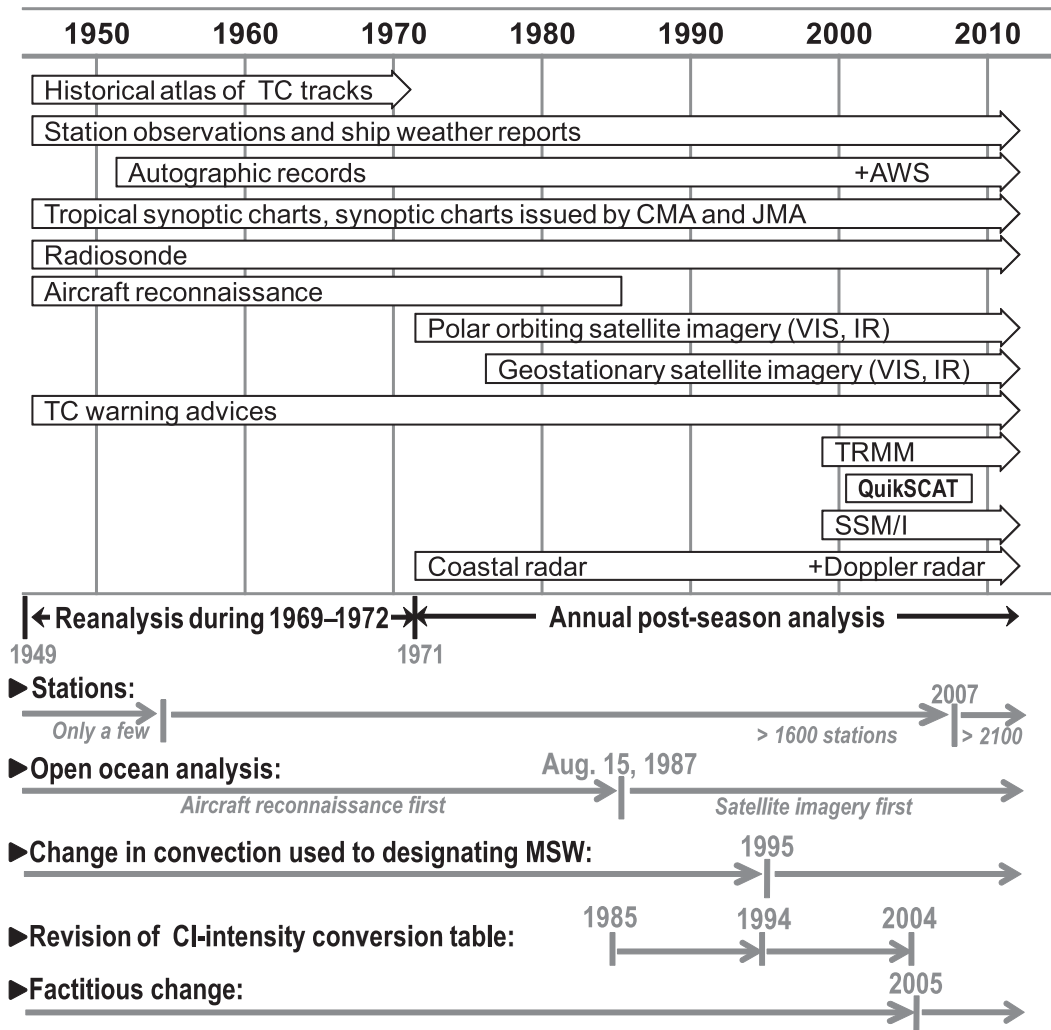


FIG. 4. Timeline (years) showing the changing sources of raw data and other important events related to the CMA TC database since 1949. AWS is the autoweather system, and JMA is the Japan Meteorological Agency.

imagery. Moreover, Fig. 6 shows that for all TCs, both over the ocean and land area, the highest MSWs occurred during the 1960s.

It can also be inferred from Fig. 6 that the convention for designating MSW has changed twice, with the MSW resolution improved for some, but not all, TCs. The most significant change was made around 1994–95, which was related to the changes in the satellite-based wind estimation table (see below). Another change occurred around 1997–98 and was related to the application of the *FengYun-2* (FY-2) satellite products. Some of these changes [e.g., the changes of convention for designating the MSW close to a threshold of TC intensity, such as TS, typhoon (TY)] may affect TC statistics when the MSW is converted to another wind averaging period (Ying et al. 2011a).

#### b. Analysis of TC best-track data

In addition to the changes in the input data, the details of the analysis procedure differ slightly between the reanalysis and postseason analysis eras. First, reanalysis begins with the identification of TC cases in historical documentation and synoptic charts, while postseason analysis begins with the identification of TD cases in addition to the real-time TC cases. When all TC cases have been identified, each case is analyzed using the ordinary subjective-based weather analysis techniques and computer-aided objective techniques, such as weather map plotting, various forms of observational data, and so on. The case-by-case analysis procedures are similar for the two eras, except that the postseason analysis has an additional step (Fig. 7)—that is, the best-track data

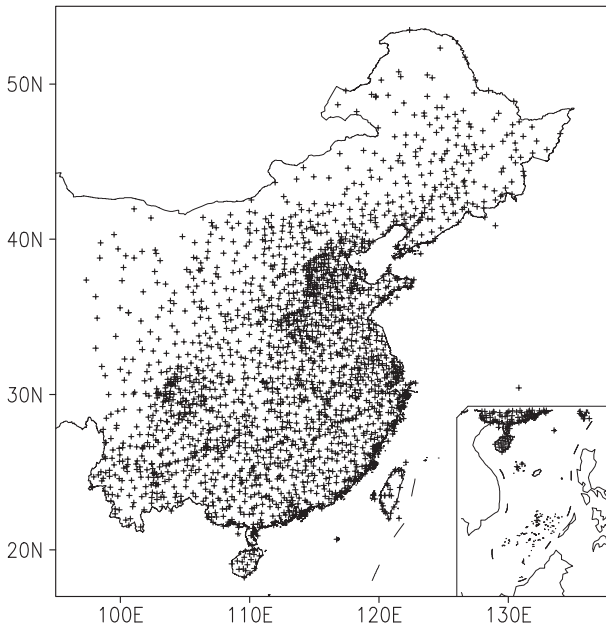


FIG. 5. Distribution of the 2153 candidate stations (+) used in the CMA TC-induced wind and precipitation dataset. The inset shows the distribution of candidate stations on the islands of the SCS.

are discussed and sanctioned at the working meeting of the CMA Workgroup on Typhoon and Marine Meteorology (WGTMM). Discussions during the working meeting focus on analysis difficulties with positions, intensities, landfall locations, and TD cases to be included in the database.

Some principles are predefined for analysis of the draft best-track data. In general, the best-track data are smoothed to reduce unrealistically abrupt changes in either track or intensity over the 6-, 12-, 18-, and 24-h periods. Keeping this in mind, different principles are applied when analyzing TCs over land or ocean, due to differences within the input data. In particular, over the ocean area, the best track is usually determined primarily according to either in situ observations or satellite images, while over the land area, the locations and intensities are analyzed based on station observations. The in situ observations include aircraft reconnaissance over the open ocean, radar over the coastal and land area, and from stations and radiosonde over land. The basic meteorological elements used in the analysis include temperature, wind, pressure, precipitation, etc. It is worth mentioning that an analysis of the evolution of the rainfall pattern accompanying a TC is helpful for fixing its position over land (see the example in section 3c).

Aircraft reconnaissance measurements were the preferred source of data over the open ocean during the period before August 1987. Other in situ observations, such as ship reports and observations from islands, may

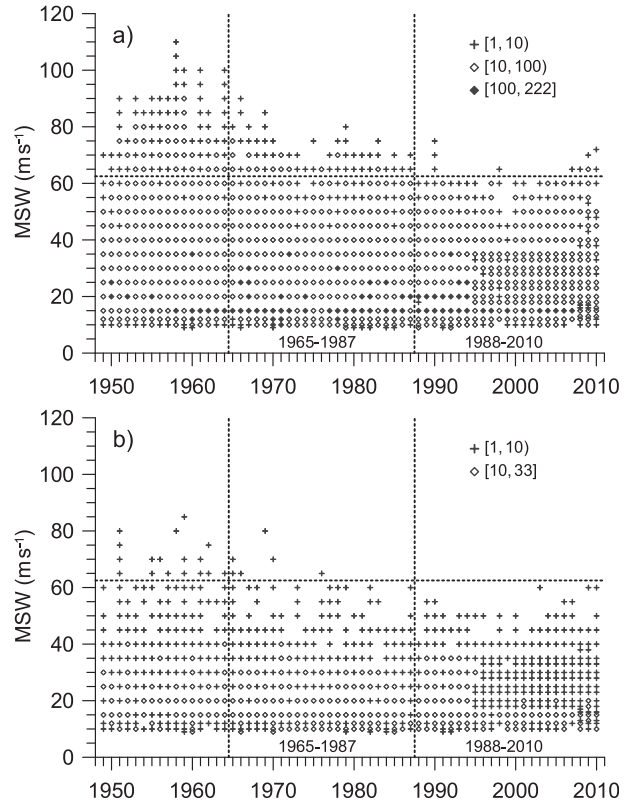


FIG. 6. Annual occurrence frequency of MSW values (denoted by a different symbol for each range interval indicated in the panels) for (a) TCs over the open ocean (i.e., at least 200 km away from any land, including islands), and (b) TCs over land (i.e., no more than 20 km away from land, including islands). The vertical dotted lines separate the two periods: 1965–87 and 1988–2010. The horizontal dotted line partitions the MSW below and above  $60 \text{ ms}^{-1}$ .

have also been important when aircraft reconnaissance data were unavailable. In fact, aircraft reconnaissance data could only cover a small part of a given TC's life span, but they were valuable over the open ocean, where other observations were unavailable. Since the end of aircraft reconnaissance missions, satellite imagery has been the preferred source of supporting data when in situ observations are unavailable.

For TCs over the land area of China, both the MSLP and MSW are recorded according to the observations. For TCs over the ocean, during the aircraft reconnaissance period before 1987 (Fig. 4), the reconnaissance data, among all available in situ observations, were preferred for intensity estimation, while other available in situ observations, such as ship reports and island observations, served as cross references and alternative sources of information. After aircraft reconnaissance was canceled, satellite imagery became the preferred choice for TCs over the open ocean, where other in situ observations

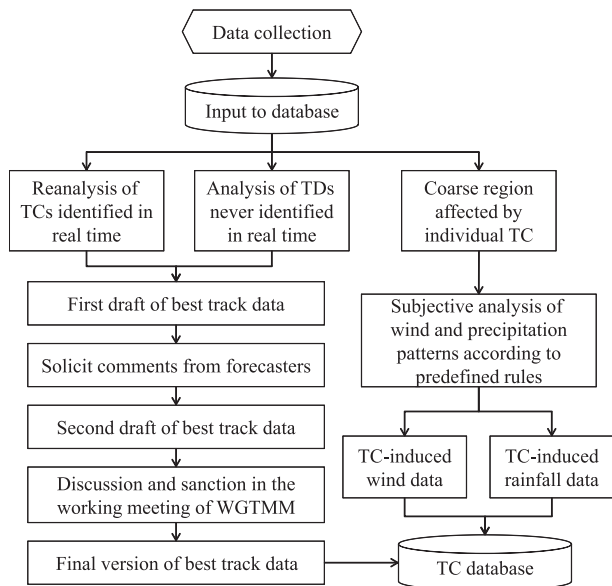


FIG. 7. Postseason analysis procedure for the CMA TC database.

were unavailable. Real-time TC warning advice is also preferred when other observations are unavailable. It should also be noted that while the wind averaging time of the MSW in the CMA best-track dataset is usually 2 min, the aircraft reconnaissance wind was observed at 1-min intervals and was not converted to a 2-min basis. This is reasonable, since the conversion factor of the two different sustained wind speeds is about 1.0 over the open ocean (Harper et al. 2010).

Either measure of TC intensity, the MSLP or MSW, may be derived from the other based on the wind–pressure relationship (WPR, see the following subsection). During the aircraft reconnaissance era, the WPR was used for the break time of reconnaissance: the MSLP is determined (by interpolation or estimation from other in situ observations) and the MSWs were then estimated according to the WPR. For satellite image analysis, the MSW is obtained from the CI number, which is estimated from cloud pattern analysis (Dvorak 1975; Group of Satellite Imagery Analysis 1980a,b), and the MSLP is then obtained according to the WPR. This introduces two important issues that are closely related to the quality of TC intensity estimation—that is, the WPR and CI–intensity conversion tables, both of which are introduced below. In addition, analysis of the extratropical transition is also presented.

1) WIND–PRESSURE RELATIONSHIP

In general, the WPR is an empirical relationship and has large uncertainties associated with it (Knaff and Harper 2010). The WPR for the CMA TC database was

TABLE 3. MSW–MSLP conversion table adopted for the annual postseason analysis of the CMA TC best-track data since the 1972 season.

MSW (m s <sup>-1</sup> )	MSLP (hPa)	MSW (m s <sup>-1</sup> )	MSLP (hPa)	MSW (m s <sup>-1</sup> )	MSLP (hPa)
12	1002	33	975	60	930–920
15	1000	35	970	65	915–910
18–20	995	40	965–960	70	905–900
23–25	990	45	955–950	75	890–895
28	985	50	945–940	80	880–885
30	980	55	935		

mainly based on a series of studies by the JTWC (JTWC 1961, 1965, 1969; Operational Department of China Central Meteorological Administration 1980) and has been changed twice. For the reanalysis era (1949–71), the WPR for the CMA best-track data is a set of latitude-dependent regression equations based on the in situ observations and the results can be inferred from Fig. 8. For the annual postseason analysis era (1972–present), the WPR is based on Table 3. As shown in Fig. 8, the WPR changed by a large amount from the reanalysis era to the annual postseason analysis era.

Note that Fig. 8 incorporates both observation-based data (i.e., aircraft reconnaissance and weather station observations) and estimated data (e.g., satellite image analysis). With respect to the WPR, the two sources of data are not equally reliable. Also, the WPR may obey different rules for the tropical and extratropical cyclone stages.

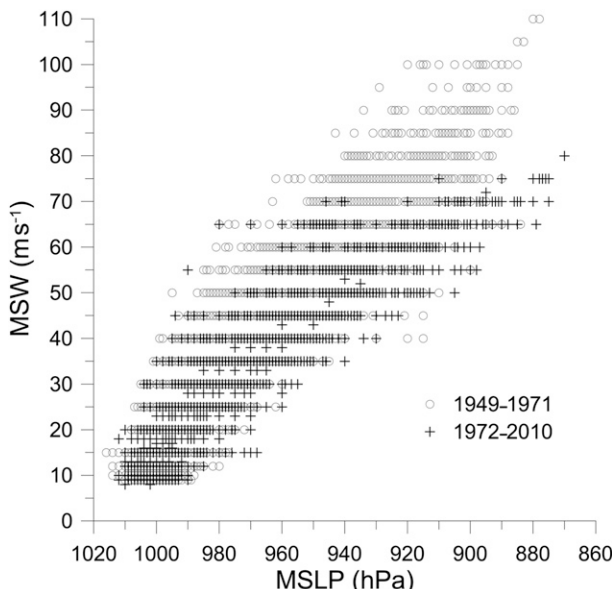


FIG. 8. Scatterplot of the WPR from the CMA best-track data. The gray open circles represent data from the 1949–71 seasons (the reanalysis era), and black crosses represent data from the 1972–2010 seasons (the postseason analysis era).

TABLE 4. Conversion table for the satellite-derived CI number and MSW used in the satellite image data analysis for the CMA TC database. The numbers in bold emphasize changes in the CI–MSW relationship between the periods 1985–93 and 1994–2004. See text for details.

CI	MSW ( $\text{m s}^{-1}$ )	
	1985–93	1994–2004
1.5	13	13
2.0	15	15
2.5	18	18
<b>3.0</b>	<b>20</b>	<b>23</b>
3.5	28	28
<b>4.0</b>	<b>30</b>	<b>33</b>
4.5	39	39
<b>5.0</b>	<b>43</b>	<b>46</b>
5.5	52	52
<b>6.0</b>	<b>56</b>	<b>59</b>
6.5	65	65
7.0	72	72
7.5	79	79
8.0	87	87

## 2) CI–INTENSITY CONVERSION TABLE

As mentioned above, in the CMA TC database, the CI number is available between 1985 and 2004 and is not the “best analysis.” Methods similar to the Dvorak technique (Group of Satellite Imagery Analysis 1980a,b) continued to be used in the annual postseason analysis for TCs over the ocean. For the 1985–2004 seasons, Table 4 summarizes the CI–MSW conversion table, which was extracted directly from the real-time satellite image analysis data. For some of the CI numbers, the corresponding MSW values were changed from the period 1985–93 to the period 1994–2004—that is, they were returned to the original Dvorak (1975) table. Unfortunately, the reasons for these changes were not documented. It is worth noting that, as can be inferred from Fig. 6a, the best-track data are based on the original Dvorak CI–MSW relationship from the 1995 season onward, coinciding with the appearance of special MSW values in Table 4 (e.g., 23 and  $33 \text{ m s}^{-1}$ ). It can also be inferred from comparison between Fig. 6a and Table 4 that the Dvorak CI–MSW relationship was not used exclusively throughout the best-track analysis, as the nontypical MSW values coexist with the typical Dvorak MSW values.

## 3) EXTRATROPICAL TRANSITION

During the reanalysis era (1949–71), the ET process was defined according to multilevel synoptic charts, and satellite imagery has been included since the 1972 season. The criterion used to indicate the end of the ET process is whether the midlatitude front system has

merged into the inner core of the TC circulation. The midlatitude front system is usually defined using either upper-level synoptic charts or satellite imagery, while the TC circulation is usually based on either surface-level or low-level synoptic charts. After the ET process, an analysis of the central location is usually conducted according to upper-level synoptic charts, such as the 850-hPa charts. The procedure is similar to that for midlatitude cyclones, including the occlusion stage. The extratropical cyclone intensity is determined from surface station observations or is estimated from synoptic charts and satellite imagery when observations are not available.

### c. Analysis of TC-induced wind and precipitation

The analysis of TC-induced wind and precipitation over the land area of China is another important issue for the CMA TC database. Approximately 2100 candidate stations have been included in the database since 2007 (Fig. 5), as compared with approximately 1600 stations in the 1980s and 1990s, and even fewer during the early 1950s (see section 3a). The change in the number of stations was mainly due to the development of the observation network in China (Ying and Wan 2011). Based on these station observations, the wind and precipitation patterns associated with TCs are determined from either synoptic charts or satellite imagery. The wind and precipitation generated by the TCs can then be determined (refer to the right side of Fig. 7).

It is well known that the interaction of TCs with other synoptic systems is quite complex over the land area of China (e.g., Chen and Ding 1979; Lei and Chen 2001). Several rules have been defined to facilitate the distinction between wind and precipitation generated by TCs and that associated with other systems. However, subjective analysis is still necessary to deal with the unique state of individual cases, which cannot be addressed according to predefined rules.

Above all, either severe wind or precipitation induced by interactions between TCs and other systems should be included in the database. This is a crucial rule and was created to ensure that more comprehensive TC data were included. Specific rules have also been established to define which interactions between a TC and various synoptic systems should be considered TC-associated. These rules are as follows.

- 1) When a TC interacts with an adjacent frontal system, the wind and precipitation on the warm airmass side are defined as TC associated.
- 2) When a TC's inverted trough interacts with a midlatitude trough, the dramatically enhanced rainfall present before the trough, the so-called remote TC

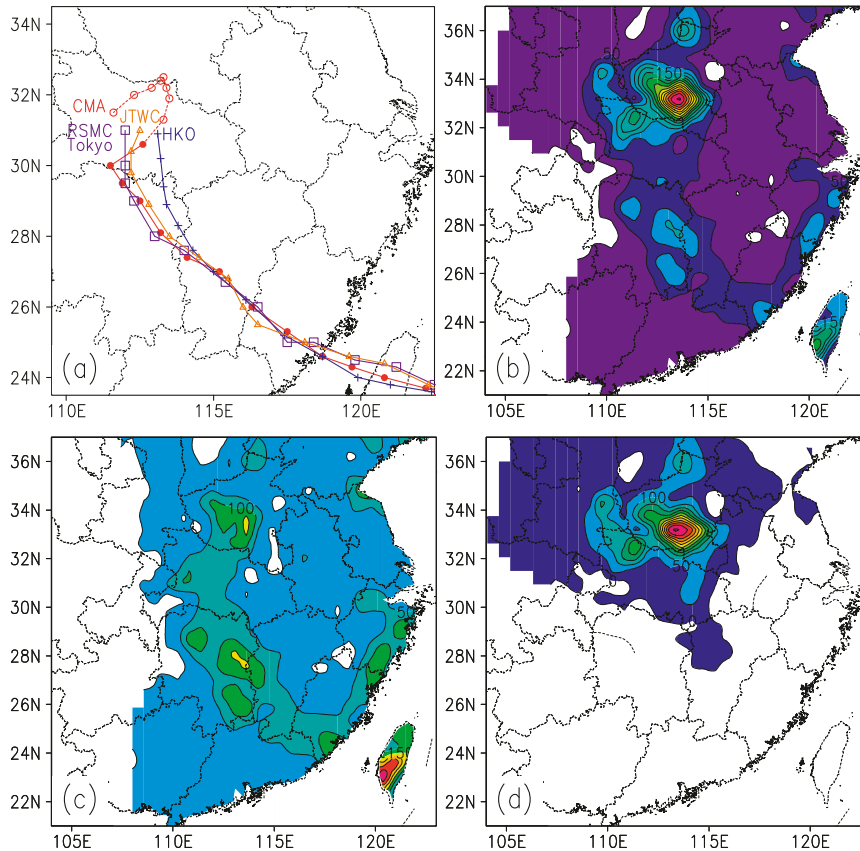


FIG. 9. Track and precipitation of Super Typhoon Nina (1975). (a) Tracks from different best-track datasets: the open and closed dots denote CMA data, “+” denotes HKO data, open triangles denote JTWC data, and open squares denote RSMC Tokyo data. Precipitation data are from the CMA TC wind and precipitation dataset. The final closed dot indicates 0000 UTC 6 Aug, which is the time that the tracks end in the HKO, JTWC, and RSMC Tokyo datasets. The dashed line with open dots indicates a track segment from the CMA data, which ends at 0000 UTC 8 Aug and is unrecorded in any other datasets. (b) Total precipitation (mm). Precipitation for (c) 1–5 and (d) 6–8 Aug (mm). The daily precipitation is calculated from 0000 to 2359 UTC (see text in section 2b). Contours for (b)–(d) are at intervals of 50 mm.

torrential rain (Chen et al. 2010; Chen and Ding 1979), is defined as TC associated.

- 3) When a TC interacts with the southwestern vortex (Kuo et al. 1986; Lu 1986; Wang and Orlanski 1987), the precipitation within the vortex circulation should be excluded from TC-associated precipitation, since the vortex itself is a rain-bearing system.
- 4) When a TC moves into the midlatitudes with a circulation absent at the surface but clear at 850–700 hPa, its precipitation is also defined as TC associated.

To minimize uncertainties, the thresholds for wind and precipitation were also defined—that is, for an individual station, the TC-associated wind is defined as wind speeds in excess of  $10.8 \text{ m s}^{-1}$ , while associated precipitation includes totals of 10 mm or more. Therefore, the duration of TC-associated wind for an individual station is defined

as extending from the first day to the last day on which observed TC-associated wind exceeds this threshold. In contrast, the duration of TC-associated precipitation for an individual station is defined according to the total precipitation and includes a 1-day addition during which the TC circulation moves away. The rule for determining the end of the TC-associated precipitation results from experience based on most of the TC cases from the early years of the database.

Figure 9 shows the example of Super Typhoon Nina (1975), which is one of the most destructive typhoons ever recorded and it caused extreme torrential rainfall and widespread destruction in China (Chen et al. 2010). Figure 9a shows the discrepancies among the Nina tracks from the four datasets listed in Table 1. In addition to the track discrepancy at each 6-h interval, the track from the CMA database is 2 days longer than that

from the other three datasets—that is, the track from the CMA database stops within Hubei Province (near  $30^{\circ}$ – $32^{\circ}$ N,  $110^{\circ}$ – $115^{\circ}$ E) at 0000 UTC 8 August 1975, while tracks from the other datasets end at 0000 UTC 6 August 1975. Figure 9b shows the total precipitation for 1–8 August generated by Nina, with the precipitation maximum in Henan Province (near  $32^{\circ}$ – $35^{\circ}$ N,  $111^{\circ}$ – $116^{\circ}$ E). It can be inferred from Figs. 9c,d that precipitation during the period 6–8 August contributed a significant proportion of this precipitation maximum. As mentioned in section 3b, the CMA included the additional track segment (shown by the dashed line and open dots in Fig. 9a) with evidence of the amplified rainfall accompanying the decaying vortex of Nina.

#### d. Reliability assessment

As the raw data sources and analysis procedures changed temporally and spatially, the reliability of the data also changed, especially in the best-track dataset. For instance, the annual TC number may not be reliable prior to the satellite era, as some TCs over the open ocean could have remained undetected. Although satellite images were not used in the reanalysis stage covering seasons from 1949 to 1971, other sources of data, such as the real-time TC warning advice issued by various agencies and the JTWC annual reports, were used to determine the candidate TC cases for reanalysis. Therefore, the annual TC number, as with the other agencies, may be reliable during the entire satellite era, including seasons before 1987.

The TC location and intensity data are in a more complex situation over the ocean. During the aircraft reconnaissance era, the reconnaissance data covered only limited periods of the TC lifespan. Accordingly, the TC location and intensity data are only reliable during those periods in which the reconnaissance data were collected. However, the MSLP from the reconnaissance data was more accurate than the wind estimation, as there were large uncertainties in both approaches used for estimating the MSW (i.e., based on the observed sea state when the sea could be seen, and derived from the aircraft flight-level winds). A recent study further suggested that the aircraft reconnaissance wind speed may be unreliable (Knapp et al. 2013). In contrast, during the satellite era (after airborne reconnaissance ended in 1987), the MSW has been estimated from satellite images using the Dvorak-type techniques, and the MSLP is then obtained by conversion from the MSW. Therefore, the MSW estimation is reasonable, while the reliability of MSLP is much lower than that from aircraft reconnaissance due to the influence of the errors in both wind estimation and WPR.

Over the land area, both MSW and MSLP are very reliable, as they are derived from in situ observations.

However, the data are inhomogeneous due to the ongoing development of the observation network. Consequently, and keeping these data inhomogeneities in mind, the TC landfall data and the TC-induced wind and precipitation data are all reliable.

#### 4. Concluding remarks

In this article, we have outlined the general features of the CMA TC database. This database focuses on TC-induced wind and precipitation observations and on some additional TC-associated phenomena that may be of interest for research purposes, such as landfall data, extratropical transitions, and subcenters, as well as outer-range and coastal severe winds. Some applications of the CMA TC database can be found in Ding and Li (2011), Dong et al. (2010), STI (1990), Xu (2006), Yang and Lei (2004), and Ying et al. (2011b,c). These data are available from STI/CMA (and via <http://tcdata.typhoon.gov.cn/en/index.html>).

In addition, the reliability of the data and potential sources of inhomogeneities within the data were also discussed in this paper. The CMA TC database contains spatial and temporal inhomogeneities, as do other similar datasets. In general, the quality of the CMA best-track data is higher over China's land and marginal sea areas than over the open ocean due to different observation densities. The changes in observation techniques influence both the best-track and TC-induced wind and precipitation data, including their temporal homogeneity, and the main events in this context are summarized in Fig. 4. The most significant changes may have been the development of the observation network over the land area, and the switch from using aircraft reconnaissance data to satellite imagery over the open ocean. Furthermore, some changes in technique may have also influenced the homogeneity of the CMA TC database, such as the change in convention for designating MSW values (Ying et al. 2011a), the revision of the CI–intensity conversion table, and factitious changes (i.e., cancellation of some of the content of the database). One of the main challenges remaining is how best to compensate for the inhomogeneities within the best-track data.

*Acknowledgments.* We sincerely thank Dr. Ken Knapp of the National Climatic Data Center and two anonymous reviewers for their constructive comments on an earlier version of the manuscript, which helped to improve the science and presentation of this study. We also thank meteorological observers, forecasters, and experts from within and outside of CMA, who were and are devoted to the construction of the database, for their hard work on data collection, processing, and analysis.

This work was supported jointly by the National Basic Research Program of China Grant 2012CB956003, the National Natural Science Foundation of China Grant 41075071, and the China National Special Funding Project for Meteorology Grant GYHY201006008.

## REFERENCES

- Chen, L., and Y. Ding, 1979: *An Introduction to West Pacific Typhoons* (in Chinese). Chinese Science Press, 491 pp.
- , Y. Li, and Z. Cheng, 2010: An overview of research and forecasting on rainfall associated with landfalling tropical cyclones. *Adv. Atmos. Sci.*, **27**, 967–976.
- Dare, R. A., and J. L. McBride, 2011: The threshold sea surface temperature condition for tropical cyclogenesis. *J. Climate*, **24**, 4570–4576.
- Diamond, H. J., A. M. Lorrey, and J. A. Renwick, 2013: A southwest Pacific tropical cyclone climatology and linkages to the El Niño–Southern Oscillation. *J. Climate*, **26**, 3–25.
- Ding, D., and Y. Li, 2011: A study on typhoon-induced rainfall over Beijing: Statistics and case analysis. *Acta Meteor. Sin.*, **25**, 742–753.
- Dong, M., L. Chen, Y. Li, and C. Lu, 2010: Rainfall reinforcement associated with landfalling tropical cyclones. *J. Atmos. Sci.*, **67**, 3541–3558.
- Dvorak, V. F., 1975: Tropical cyclone intensity analysis and forecasting from satellite imagery. *Mon. Wea. Rev.*, **103**, 420–430.
- Emanuel, K. A., 2005: Increasing destructiveness of tropical cyclones over the past 30 years. *Nature*, **436**, 686–688.
- Gao, Y., and Y. Zeng, 1957: *Atlas on Typhoon Tracks and Statistics* (in Chinese). Chinese Science Press, 136 pp.
- Group of Satellite Imagery Analysis, 1980a: Methods for typhoon prediction using the satellite imagery (I) (in Chinese). *Meteor. Mon.*, **6**, 24–26.
- , 1980b: Methods for typhoon prediction using the satellite imagery (II) (in Chinese). *Meteor. Mon.*, **6**, 25–27.
- Harper, B. A., J. D. Kepert, and J. D. Ginger, 2010: Guidelines for converting between various wind averaging periods in tropical cyclone conditions. World Meteorological Organization Tech. Doc. WMO/TD-1555, 54 pp.
- Hoarau, K., L. Chalonge, and J. P. Hoarau, 2006: The reasons for a reanalysis of the typhoon's intensity in the western North Pacific. Preprints, *27th Conf. on Hurricanes and Tropical Meteorology*, Monterey, CA, Amer. Meteor. Soc., 5B.2. [Available online at [https://ams.confex.com/ams/27Hurricanes/techprogram/paper\\_109050.htm](https://ams.confex.com/ams/27Hurricanes/techprogram/paper_109050.htm).]
- Holland, G. J., Ed., 1993: Global guide to tropical cyclone forecasting. WMO Tech. Doc. WMO/TD-560, Tropical Cyclone Programme Rep. TCP-31. [Available online at [http://www.cawcr.gov.au/publications/BMRC\\_archive/tcguide/globa\\_guide\\_intro.htm](http://www.cawcr.gov.au/publications/BMRC_archive/tcguide/globa_guide_intro.htm).]
- Knaff, J. A., and B. A. Harper, 2010: Tropical cyclone surface wind structure and wind-pressure relationships. *Seventh Int. Workshop on Tropical Cyclones*, La Réunion, France, WMO, KN1. [Available online at <http://www.wmo.int/pages/prog/arep/wwrp/tmr/otherfileformats/documents/KN1.pdf>.]
- Knapp, K. R., M. C. Kruk, D. H. Levinson, H. J. Diamond, and C. J. Neumann, 2010: The International Best Track Archive for Climate Stewardship (IBTrACS): Unifying tropical cyclone data. *Bull. Amer. Meteor. Soc.*, **91**, 363–376.
- , J. Knaff, C. Sampson, G. Riggio, and A. Schnapp, 2013: A pressure-based analysis of the historical western North Pacific tropical cyclone intensity record. *Mon. Wea. Rev.*, **141**, 2611–2631.
- Kuo, Y.-H., L. Cheng, and R. A. Anthes, 1986: Mesoscale analysis of the Sichuan flood catastrophe, 11–15 July 1981. *Mon. Wea. Rev.*, **114**, 1984–2003.
- Kwon, H.-J., S.-H. Won, and S.-K. Park, 2006: Climatological differences between the two typhoon centers' tropical cyclone information in the western North Pacific. *J. Korean Meteor. Soc.*, **42**, 183–192.
- Lander, M. A., 2008: A comparison of typhoon best-track data in the western North Pacific: irreconcilable differences. Preprints, *28th Conf. on Hurricanes and Tropical Meteorology*, Orlando, FL, Amer. Meteor. Soc., 4B.2. [Available online at [https://ams.confex.com/ams/28Hurricanes/techprogram/paper\\_137395.htm](https://ams.confex.com/ams/28Hurricanes/techprogram/paper_137395.htm).]
- , and C. P. Guard, 2006: The urgent need for a re-analysis of western North Pacific tropical cyclones. Preprints, *27th Conf. Hurricanes and Tropical Meteorology*, Monterey, CA, Amer. Meteor. Soc., 5B.3. [Available online at <https://ams.confex.com/ams/pdfpapers/107845.pdf>.]
- Landsea, C. W., B. A. Harper, K. Hoarau, and J. A. Knaff, 2006: Can we detect trends in extreme tropical cyclones? *Science*, **313**, 452–454.
- Lee, T.-C., T. R. Knutson, H. Kamahori, and M. Ying, 2012: Impacts of climate change on tropical cyclones in the western North Pacific basin. Part I: Past observations. *Trop. Cyclone Res. Rev.*, **1**, 213–230.
- Lei, X., 2001: The precision analysis of the best positioning on WNP TC (in Chinese). *J. Trop. Meteor.*, **17**, 65–70.
- , and L. Chen, 2001: Tropical cyclone landfalling and its interaction with mid-latitude circulation systems (in Chinese). *Acta Meteor. Sin.*, **59**, 602–615.
- Levinson, D. H., H. J. Diamond, K. R. Knapp, M. C. Kruk, and E. J. Gibney, 2010: Toward a homogenous global tropical cyclone best-track dataset. *Bull. Amer. Meteor. Soc.*, **91**, 377–380.
- Lu, J., 1986: *Introduction to the Southwest Vortex* (in Chinese). China Meteorological Press, 270 pp.
- Meng, Z., M. Nagata, and L. Chen, 1996: A numerical study on the formation and development of island-induced cyclone and its impact on typhoon structure change and motion. *Acta Meteor. Sin.*, **10**, 430–443.
- Nakazawa, T., and S. Hoshino, 2009: Intercomparison of Dvorak parameters in tropical cyclone datasets over the western North Pacific. *SOLA*, **5**, 33–36.
- Onogi, K., and Coauthors, 2007: The JRA-25 Reanalysis. *J. Meteor. Soc. Japan*, **85**, 369–432.
- Operational Department of China Central Meteorological Administration, Ed., 1980: *Reference Manual on Typhoon Reconnaissance Report and Warning Message* (in Chinese). China Meteorological Press, 117 pp.
- Peterson, T. C., and Coauthors, 1998: Homogeneity adjustments of in situ atmospheric climate data: A review. *Int. J. Climatol.*, **18**, 1493–1517.
- Reade, D., 2011: Storm hunters: The navy's hurricane reconnaissance units. *Naval Aviation News*, Vol. 94, Naval Aviation News, Patuxent River, MD, 14–19.
- Shanghai Typhoon Institute, 1990: *Climatological Atlas for Northwest Pacific Tropical Cyclones*. China Meteorological Press, 316 pp.
- Wang, B., and I. Orlanski, 1987: Study of a heavy rain vortex formed over the eastern flank of the Tibetan Plateau. *Mon. Wea. Rev.*, **115**, 1370–1393.

- Wang, L., 1997: *Shanghai Meteorological History* (in Chinese). Shanghai Social Science Press, 715 pp.
- Wang, X., L. Wu, F. Ren, Y. Wang, and W. Li, 2008: Influences of tropical cyclones on China during 1965-2004. *Adv. Atmos. Sci.*, **25**, 417-426.
- Wu, M. C., K. H. Yeung, and W. L. Chang, 2006: Trends in western North Pacific tropical cyclone intensity. *Eos, Trans. Amer. Geophys. Union*, **87**, 537-548.
- Xu, Y., Ed., 2006: *Climatological Atlas for Tropical Cyclones Affecting China (1951-2000)*. Science Press, 177 pp.
- Yang, Y., and X. Lei, 2004: Statistics of strong wind distribution caused by landfall typhoon in China (in Chinese). *J. Trop. Meteor.*, **6**, 633-642.
- Ying, M., and R. Wan, 2011: The annual frequency prediction of tropical cyclones affecting China (in Chinese). *J. Appl. Meteor. Sci.*, **22**, 66-76.
- , E.-J. Cha, and H. J. Kwon, 2011a: Comparison of three western North Pacific tropical cyclone best track datasets in a seasonal context. *J. Meteor. Soc. Japan*, **89**, 211-224, doi:10.2151/jmsj.2011-303.
- , B. Chen, and G. Wu, 2011b: Climate trends in tropical cyclone-induced wind and precipitation over mainland China. *Geophys. Res. Lett.*, **38**, L01702, doi:10.1029/2010GL045729.
- , Y. Yang, B. Chen, and W. Zhang, 2011c: Climatic variation of tropical cyclones affecting China during the past 50 years. *Sci. China Earth Sci.*, **54**, 1226-1237, doi:10.1007/s11430-011-4213-2.
- , G. Wu, Y. Liu, and S. Sun, 2012: Modulation of land-sea thermal contrast on the energy source and sink of tropical cyclone activity and its annual cycle. *Sci. China Earth Sci.*, **55**, 1855-1871, doi:10.1007/s11430-012-4421-4.
- Yu, H., C. Hu, and L. Jiang, 2007: Comparison of three tropical cyclone intensity datasets. *Acta Meteor. Sin.*, **21**, 121-128.
- , Y. Lu, P. Chen, and W. Zhou, 2012: Intensity change characteristics of tropical cyclones in the western North Pacific as revealed by three different datasets. *J. Trop. Meteor.*, **18**, 119-126.